RETROGRADE MAPPING OF INPUTS TO DIRECT- AND INDIRECT-PATHWAY NEURONS IN THE POSTERIOR DORSOMEDIAL STRIATUM

An Undergraduate Research Scholars Thesis

by

BRITTON RAE BARBEE

Submitted to the Undergraduate Research Scholars program at
Texas A&M University
in partial fulfillment of the requirements for the designation as an

UNDERGRADUATE RESEARCH SCHOLAR

Approved by Research Advisor: Dr. Jun Wang

May 2017

Major: Molecular and Cell Biology

TABLE OF CONTENTS

ABSTRACT

Retrograde Mapping of Inputs to Direct- and Indirect-pathway Neurons in the Posterior Dorsomedial Striatum

Britton Rae Barbee
Department of Biology
Texas A&M University

Research Advisor: Dr. Jun Wang
Department of Neuroscience and Experimental Therapeutics
Texas A&M University

The dorsomedial striatum (DMS) is crucial for goal-directed learning and heavily implicated in drug and alcohol addiction. The posterior DMS (pDMS) receives multiple inputs and contains medium spiny neurons (MSNs) expressing dopamine D1 receptors (D1Rs) or D2Rs. These neurons exhibit abnormal synaptic plasticity after excessive alcohol consumption. However, the different sources of the afferent inputs to pDMS D1- vs. D2-MSNs are unclear. To identify the presynaptic neurons projecting to specific neuronal types, we used a state-of-the-art monosynaptic retrograde tracing technology to label these presynaptic neurons in the whole mouse brain. Then, we determined the extent to which those presynaptic cells projecting to pDMS D1-MSNs (or D2-MSNs) also contain D1Rs (or D2Rs). We found abundant projecting neurons in the different cortical regions, amygdala, thalamus, and midbrain. Interestingly, we found that most D1-MSN-projecting neurons did not express D1Rs; most D2-MSN-projecting neurons did not express D2Rs. We only observed a few D1-MSN-projecting neurons in the cortex and thalamus contained D1Rs; a few D2-MSN-projecting neurons in the cortex, thalamus, and midbrain neurons expressed D2Rs. These results suggest that connected corticostriatal and

thalamostriatal neurons do not express the same type of dopamine receptors, which is an important question in the addiction field that has not been addressed before. Understanding these connections will also improve our knowledge of the pDMS circuit in drug addiction.

DEDICATION

To my parents, Kevin and Rhonda Barbee, for their continuous and unyielding support of my education. I owe everything to them.

ACKNOWLEDGEMENTS

I want to thank my faculty advisor, Dr. Jun Wang, for his continuous guidance and support throughout my time in the lab, especially on this project. I also want to recognize my graduate student advisor, Yifeng Cheng, for his technical support and direction. I am grateful for the other members of the lab, specifically Dr. Xuehua Wang for her patience and teaching, as well as the other undergraduates, Jared Jerger, Sebastian Melo, Nathaniel Teplitskiy, Caroline Matlock, and Eric Williams. Without them, this would have been impossible.

NOMENCLATURE

DMS	Dorsomedial Striatum
pDMS	Posterior dorsomedial striatum
aDMS	Anterior dorsomedial striatum
D1-MSNs	Dopamine D1-receptor expressing medium spiny neurons
D2-MSNs	Dopamine D2-receptor expressing medium spiny neurons
OFC	Orbitofrontal cortex
PFC	Medial frontal cortex
BLA	Basolateral amygdala
SNc	Substantia nigra pars compacta

CHAPTER I

INTRODUCTION

Alcohol use disorder is a devastating disease that levies a damaging burden to our society, both economically and socially. In 2010, excess alcohol consumption incurred a cost of almost $250 billion, with 40.4% paid for by the United States government (Sacks et al., 2015). Excessive consumption also resulted in 9.8% of premature deaths in the United States from 2006-2010, with most chronic and acute deaths from alcoholic liver disease and motor vehicle accidents, respectively (Stahre et al., 2014). To lessen these detrimental effects, a more advanced understanding of the alterations within neuronal pathways associated with the disorder is crucial for developing therapeutic interventions and eventually a cure.

The basal ganglia are a collection of subcortical nuclei that are innervated by dopaminergic neurons and are implicated in voluntary movement, as well as habitual and procedural learning (Bolam et al., 2000; Joel and Weiner, 2000; Gerfen and Surmeier, 2011). The striatum is the main input of the basal ganglia and can be divided into the dorsal and ventral striatum (Voorn et al., 2004). The dorsal striatum can be further divided into the dorsomedial striatum (DMS), which is involved in action-outcome associative learning in goal directed behaviors, and the dorsolateral striatum, which contributes to habit formation (Joel and Weiner, 2000; Voorn et al., 2004; Tricomi et al., 2009; Wang et al., 2010). Importantly, excessive alcohol consumption induces aberrant structural and synaptic plasticity change (Wang et al., 2010; Wang et al., 2015; Cheng et al., 2016). The principal cells of the DMS are medium spiny neurons (MSNs) that can be subdivided into dopamine D1 receptor-expressing MSNs (D1-MSNs) and

dopamine D2 receptor-expressing MSNs (D2-MSNs) (Volkow and Morales, 2015). The D1-MSNs project to the substantia nigra pars reticulata (SNr), forming the direct pathway and controlling "Go" actions (Gerfen and Surmeier, 2011; Sippy et al., 2015; Volkow and Morales, 2015; Wang et al., 2015). The D2-MSNs connect to the SNr via the external globus pallidus and subthalamic nucleus, giving rise to the indirect pathway and regulating "No-Go" actions (Sano et al., 2003; Gerfen and Surmeier, 2011; Sippy et al., 2015; Volkow and Morales, 2015; Wang et al., 2015).

In addition, the DMS can be further subdivided into two regions: the anterior DMS (aDMS) and the posterior DMS (pDMS). The aDMS is a crucial location for modifying behavior in response to associative learning (Williams and Eskandar, 2006; Corbit and Janak, 2010). The pDMS is the neural substrate by which action-outcome associations are assimilated and expressed in goal-directed learning (Yin et al., 2005; Corbit and Janak, 2010; Shiflett et al., 2010). Therefore, the pDMS is likely to be a crucial region in forming the action-outcome associations that are augmented in addiction. It is known to receive inputs from the basolateral amygdala (BLA) that are necessary for goal-directed learning to occur (Corbit et al., 2013).

However, the sources of the afferent projections to the pDMS are uncertain. To map neurons projecting to specific pDMS D1- vs. D2-MSNs, we infused a monosynaptic pseudotype of the rabies virus that carries a green fluorescent protein (GFP): EnvA-SADΔG-EGFP into D1-Cre;Ai14 and D2-Cre;Ai14 transgenic mice. D1-Cre;Ai14 mice express tdTomato (red) after undergoing Cre recombinase; the Cre is restricted to D1-MSN neurons, thus, only the D1-MSNs display red. Similarly, D2-Cre;Ai14 mice express tdTomato in D2-MSNs (Lemberger et al.,

2007; Madisen et al., 2010). This method enables us to observe presynaptic neurons that project to genetically identified postsynaptic neurons in a cell-type specific manner, allowing us to determine the extent to which those cells projecting to pDMS D1-MSNs (or D2-MSNs) also contain D1 (or D2) receptors (Wickersham et al., 2007; Wall et al., 2013). Thus, it informs us whether two brain regions express the same dopamine receptors and are activated together by dopamine signaling, which has not been previously examined in addiction research. This also strengthens our understanding of the pDMS and its role in drug addiction.

CHAPTER II

METHODS

Reagents

AAV2.5-Cre-eGFP was purchased from the University of Pennsylvania School of Medicine. AAV8-Flex-RG and AAV8-Flex-TVA-mCherry helper viruses were obtained from UNC. EnvA-SADΔG-EGFP ($3x10^{-7}$ TU/mL) was purchased from the Salk Institute Vector Core. NeuroTrace Blue, Green, and NeuroTrace Red were obtained from LifeTechnologies. All other reagents were purchased from Sigma.

Animals

Drd1a-Cre (D1-Cre) and *drd2*-Cre (D2-Cre) mice were purchased from Mutant Mouse Regional Resource Centers. Ai14 and C57BL/6J mice were obtained from The Jackson Laboratory. D1-Cre and D2-Cre mice were crossed with Ai14 mice to produce D1-Cre;Ai14 and D2-Cre;Ai14 offspring, respectively. All mice were bred onto a C57BL/6J background. Mice were group housed at 23 degrees Celsius with a 12 hour light: dark cycle, lights on at 11:00 pm, with food and water provided *ad libitum*. The experimental procedures and animal care protocols were approved by the Texas A&M University Institutional Animal Care and Use Committee and were performed in agreement with the National Research Council *Guide for the Care and Use of Laboratory Animals.*

Genotyping

Genotyping was conducted in-house using a MJ Research PTC-200 Thermal Cycler (GMI, Inc, Ramsey, MN, USA) for PCR. DNA extraction was conducted using a Genotyping Sigma Kit (Sigma-Aldrich, St. Louis, MO) and primers (Sigma-Aldrich) with sequences as follows: Cre: forward 5'-GATGCAACGAGTGATGAG -3', reverse 5'-TCGGCTATACGTAACAGG-3'. Ai14 Wild Type: forward 5'-AAGGGAGCTGCAGTGGAGTA-3', reverse 5'-CCGAAAATCTGTGGGAAGTC-3'. Ai14 mutation: forward 5'-CTGTTCCTGTACGGCATGG-3', reverse 5'-GGCATTAAAGCAGCGTATCC -3'. Ai32 Wild Type: forward 5'-AAG GGA GCT GCA GTG GAG TA-3', reverse 5'-CCG AAA ATC TGT GGG AAG TC-3'. Ai32 mutation: forward 5'-ACA TGG TCC TGC TGG AGT TC-3', reverse 5'-GGC ATT AAA GCA GCG TAT CC-3'.

Surgery

For the stereotaxic viral infusions, mice were placed under isoflurane anesthesia, and mounted in a stereotax frame (Kopf). An incision was made to open the skin and uncover the skull, which was then cleaned using 30% hydrogen peroxide. The spatial coordinates were measured and drilled into, creating a small hole to expose the brain for infusion. To confirm the infusion site coordinates and retrograde labeling, two microinjectors were loaded with 0.4 µL of AAV2.5-Cre-eGFP. To prepare for the the EnvA-SADΔG-EGFP pseudorabies virus, two microinjectors were loaded with 0.6 µL of a 1:1 mixture of AAV8-Flex-RG and AAV8-Flex-TVA-mCherry.

For each infusion, the mice were bilaterally infused at a rate of 0.1 µL/min into the pDMS at adapted coordinates, measured from bregma for AP and ML, and dura for DV (Paxinos and Franklin, 2004): AP, 0.0 mm; ML, ± 1.87 mm; DV, -2.90 mm. Microinjectors were left for 10 minutes after infusion and were then removed and the skin was closed using skin glue. Meloxicam (0.1 mL/100 g body weight, s.c.) was used for pain management after surgery.

Mice were allowed to recover for four weeks, then the EnvA-SADΔG-EGFP pseudorabies virus was infused at a 10 degree angle, measured from the midline, parallel to the DV axis using adapted coordinates (AP, 0.0 mm; ML, ± 2.42 mm; DV, -2.94 mm). The angled injection prevents coincident viral infection at the injection tract while targeting the pDMS.

Histology and cell counting

After complete viral expression (1 week after rabies infusion), the mice were anesthetized using isoflurane and transcardially perfused using 4% paraformaldehyde (PFA) in phosphate-buffered saline (PBS). The brains were removed and post-fixed overnight in 4% PFA, then dehydrated using 30% sucrose. Brains were then cut into 50-µm coronal sections using a cryostat. Sections were washed in PBS and then maintained in 0.1% Triton X-100 for 10 minutes, then incubated in the dark in NeuroTrace Red for 20 minutes, or NeuroTrace Blue or Green for 30 minutes.

Confocal images were acquired using an Olympus Fluoview 1200 confocal scanning microscope. Image analysis was completed using the Bitplane Imaris software (Bitplane, Switzerland).

CHAPTER III

RESULTS

Identification of the pDMS infusion site and retrograde labeling of pDMS-projecting neurons in the BLA

We used a retrograde virus, AAV2.5-Cre-eGFP, to verify the coordinates we chose for the infusion site into the pDMS. When the virus is infused into the pDMS, the virus directly infects the neurons around the infusion site and produces fluorescence due to the Cre in the virus recombining with the fluorescence-encoding transgene present in the animal. The virus is also able to infect the axon terminals present in the pDMS, which allows the virus to retrogradely travel along the axon and infect the soma not present in the infusion site. Thus, we see bright fluorescence in the pDMS at the infusion site and in somas in different regions that project into the pDMS.

To verify the coordinate infusion site of the pDMS and retrograde labeling of DMS-projecting neurons, we infused AAV2.5-Cre-eGFP into the pDMS of Ai32 mice. The Ai32 mouse line expresses eGFP after Cre recombinase (Madisen et al., 2012). Six weeks after infusion, we perfused the animal and coronal sections were prepared with a counterstain of NeuroTrace Blue (Figure 1A) or Red. The AAV2.5-Cre-eGFP infusion in the pDMS caused a strong expression of GFP in the pDMS neurons, as well as some neurons in the cortex. Those pDMS green neurons express GFP after Cre recombinase (Madisen et al., 2012), whereas the neurons in the cortex express GFP due to retrograde transport of the Cre from the pDMS and drives GFP expression.

It has been reported that the BLA projects to the pDMS in rats using the traditional method fluorogold (Corbit and Janak, 2010). We then examined the GFP-positive neurons in the BLA, and we could not find BLA neurons (Figure 1B-C). This could be due to Ai32 having weak expression.

To further confirm the infusion sites and retrograde labeling, we infused the same virus into the pDMS of an Ai14 mouse using the same coordinates. As stated earlier, Ai14 is a mouse line that expresses a very bright fluorescent protein, tdTomato, after Cre recombinase (Madisen et al., 2010). We also detected many red neurons (tdTomato positive) in the pDMS (Figure 1D). We also observed a lot of red neurons, which might come from the direct expression of AAV2.5-Cre-eGFP. Interestingly, we observed a very strong expression of tdTomato in the BLA of this animal, which suggests that the expression in the Ai14 mouse line is stronger than the Ai32. We observed BLA neurons expressing tdTomato from the AAV2.5-Cre-eGFP retrograde (Figure 1E).

Mapping the inputs to pDMS D1-MSNs

After verifying our infusion site coordinates, we first infused AAV8-Flex-RG and AAV8-Flex-TVA-mCherry (1:1) into the pDMS of six D1-Cre;Ai14 mice and waited four weeks to allow the expression of rabies glycoprotein (RG) and TVA in D1-MSNs, which are required for the rabies viral infection to these neurons. Again, we used D1-Cre;Ai14 instead of D1-Cre mice because we want to see the overlap between pDMS-projecting neurons and those neurons that express D1Rs outside the striatum. Four weeks after the first infusion, we infused EnvA-

SADΔG-EGFP pseudorabies virus at a 10-degree angle to prevent coincident infection. One week later, the animals were perfused and coronal sections of the whole brain were prepared. Confocal images were acquired in several key brain regions. To determine whether pDMS D1-MSN-projecting neurons also contained D1Rs, we analyzed the confocal images using Imaris to detect colocalization of tdTomato-expressing neurons (red) and pseudorabies-expressing neurons (green). These overlapping neurons will appear yellow and can be detected by the program.

As we predicted, in the pDMS infusion site we observed yellow neurons, which express rabies and the D1R, as well as green neurons, which should be D2-MSNs projecting to the infected D1-MSNs (Taverna et al., 2008). In addition, we observed expression in the cortical regions: orbitofrontal cortex (OFC) (Figure 2B), dorsomedial prefrontal cortex (dmPFC) (Figure 2C), cingular cortex (Figure 2D), and motor cortex (Figure 2E). These regions are all known to provide glutamatergic inputs to the dorsomedial striatum (Tepper et al., 2007; Lovinger, 2010). Other major glutamatergic inputs, the thalamus and the BLA, showed input from thalamus (Figure 2F) but no expression in the BLA (image not shown) (Smith et al., 2004; Everitt and Robbins, 2005). In addition to these glutamatergic inputs, the D1-MSNs also receive extensive dopaminergic inputs from the midbrain (Surmeier et al., 2007). We found projecting neurons in the substantia nigra pars compacta (SNc) (Figure 2G). Lastly, it has been reported that MSNs also receive GABAergic inputs from outside the striatum (Lee et al., 2004). In fact, we found green neurons in the external segment of the globus pallidus (GPe), suggesting that D1-MSNs receive GABAergic inputs from the GPe (Figure 2H). These results suggest that pDMS D1-MSNs receive inputs from a number of brain regions outside the striatum.

Since we used D1-Cre;Ai14 animals, in which all neurons express D1Rs, including neurons outside the striatum (Wei et al., 2017), we then examined the colocalization of GFP and the tdTomato to determine whether those neurons that project to the D1-MSNs also contain D1Rs. As observed in Table 1, we detected overlap in the cingular cortex (Figure 2D, inset), the motor cortex (image not shown), and the thalamus (image not shown), which indicates that those D1-MSN-projecting neurons express D1Rs, but the remaining cortical regions, BLA, SNc, and GPe do not express D1Rs. The percentage of overlap is very low (0.5-1.8%, Table 1), indicating that D1R-expressing neurons outside the striatum are not major inputs to pDMS-D1-MSNs.

Mapping the inputs to pDMS D2-MSNs

We followed the same infusion protocol using four D2-Cre;Ai14 mice. As we expected, in the pDMS infusion site we observed abundant yellow neurons, which express rabies and the D2R, as well as green neurons, which should be D1-MSNs projecting to the infected D2-MSNs (Figure 3A) (Taverna et al., 2008). Interestingly, we detected numerous GFP-expressing neurons in cortical areas: OFC, dmPFC, cingular cortex, and motor cortex (Figures 3B-3E). We also noticed several GFP-expressing neurons in the thalamus (Figure 3F) and very limited expression in the BLA (Figure 3G). The SNc (Figure 3H) and the GPe (Figure 3I) also showed some GFP-expressing neurons. These data indicate that D2-MSNs in the pDMS receive input from a variety of brain regions other than the striatum.

We also measured the colocalization as described above. We observed low amounts of overlap in the OFC (Figure 3B, inset), cingular cortex (image not shown), motor cortex (Figure

3E, inset), the thalamus (Figure 3F, inset), and the SNc (Figure 3H, inset). The overlapping percentage ranged from 0.38 in the cingular cortex to 24.31% in the thalamus (Table 2). These results suggest that some D2R-expressing neurons outside the striatum project to pDMS D2-MSNs.

Comparing the inputs to pDMS D1- vs. D2-MSNs

To compare the different inputs to D1- vs. D2-MSNs, the number of green neurons in each brain region examined was normalized to the average number of rabies-GFP starter cells in the pDMS of either D1-Cre;Ai14 or D2-Cre;Ai14 mice (Figure 4A). For the calculation, the number of pDMS starter cells in each mouse was counted, and then the number of cells in each corresponding brain region was divided by the number of starter cells and multiplied by 100 to obtain the percentage (Figures 4B-4H). This process was repeated for each individual mouse, and then the data were averaged.

We did not observe a significant difference in the average number of starter cells between D1-Cre;Ai14 or D2-Cre;Ai14 mice (Figure 4A). Remarkably, all observed cortical regions had a substantially higher percentage of rabies-GFP-expressing neurons in the D2-Cre;Ai14 mice than in the D1-Cre;Ai14 animals (Figure 4B-4E). Interestingly, the thalamus had a slightly higher expression of rabies-GFP-expressing neurons in the D1-Cre;Ai14 mice in comparison with the D2-Cre;Ai14 mice (Figure 4F). The SNc also contained a significantly higher percentage of rabies-GFP-expressing neurons in D2-Cre;Ai14 mice (Figure 4G). The GPe of D2-Cre;Ai14 mice also contained a larger percentage of rabies-GFP-expressing neurons when compared to

D1-Cre;Ai14 mice (Figure 4H). Overall, all observed pDMS-projecting GABAergic (GPe) and dopaminergic (SNc) regions expressed more rabies-GFP neurons in D2-Cre;Ai14 animals. However, while all cortical glutamatergic regions (OFC, dmPFC, motor cortex, cingular cortex) projecting to the pDMS had a significantly higher rabies-GFP expression percentage in the D2-Cre;Ai14 animals, the thalamus, another glutamatergic projecting region to the pDMS, showed slightly more rabies-GFP expression in D1-Cre;Ai14 mice.

Additionally, we also compared the percentage of relative inputs to D1- vs. D2-MSNs. The percentage of D1R or D2R total inputs into each brain region was calculated by dividing the number of rabies-GFP neurons in that region by the number of total rabies-GFP-expressing neurons, and multiplying the result by 100 to obtain the percentage (Figure 4I). Overall, the D1-Cre;Ai14 mice had the highest percentage of total inputs to D1-MSNs in the pDMS from the thalamus, followed closely by the dmPFC and the cingular cortex. They also showed sizeable inputs from the motor cortex, the dmPFC, and the OFC. There were limited inputs from the GPe, sensory cortex, associate cortex, other cortical areas, and the SNc. Interestingly, there were no inputs to D1-MSNs from the BLA (Figure 4I, right). However, D2-Cre;Ai14 mice showed the largest percentage of total inputs to D2-MSNs in the pDMS from the motor cortex. These mice also had sizeable total inputs from the GPe, followed by the cingular cortex, dmPFC, SNc, thalamus, other cortical regions, and OFC. Remarkably, there is a small percentage of D2-MSNs in the BLA that project to D2-MSNs in the pDMS (Figure 4I, left).

CHAPTER IV

DISCUSSION

In this study, we used the monosynaptic and transsynaptic EnvA-SADΔG-EGFP pseudorabies virus paradigm to determine whether pDMS D1- and D2-MSNs have distinct extrastriatal inputs, and if so, what percentage of these extrastriatal neurons that project onto D1-MSNs (or D2-MSNs) also contain D1Rs (or D2Rs). Our results demonstrated that both pDMS D1- and D2-MSNs receive inputs from a variety of brain regions, with a greater extent to D2-MSNs than D1-MSNs. In addition, the relative inputs from different regions to pDMS D1- vs. D2-MSNs are also different. Interestingly, we did not observe high overlapping of D1R-expressing (or D2R-expressing) neurons and neurons projecting to pDMS D1-MSNs (or D2-MSNs).

In contrast to our expectations, we did not observe strong overlap between pDMS-projecting neurons and pDMS neurons expressing the same type of dopamine receptors. This indicates that the inputs to pDMS D1-MSNs are not from those D1R-expressing neurons outside the striatum. Similarly, the inputs to pDMS D2-MSNs are not from D2R-expressing neurons. These inputs include glutamatergic inputs from the cortex, thalamus, and BLA. We previously observed very strong D1R- or D2R-expressing neurons in these areas (Wei et al., 2017). Lack of overlapping suggests that those pDMS D1-projecting neurons do not contain D1Rs; similarly, pDMS D2-projecting neurons do not express D2Rs. It would be interesting to test whether those pDMS D1-MSN projecting cortical neurons possess another receptor type, such as D2Rs. We were

unsurprised that GABAergic projections from the GPe did not show any overlap, because these neurons do not express either D1Rs or D2Rs (Lee et al., 2004).

The SNc is known to project to the DMS and has been shown to primarily contain D2-MSNs that contain autoreceptors (Wei et al., 2017); we did observe SNc neurons projecting to D2-MSNs. Therefore, it can be used as a positive control for verification of the surgical technique, since there should be no overlap in D1-Cre;Ai14 mice. We found some overlap in the SNc, indicating that the surgeries were successful in selectively identifying pDMS-projecting D2-MSNs. The overlap was not 100%, however, it has been suggested that the pseudotyped rabies strain is limited in its ability to traverse the space between the dendrites juxtaposed to dopaminergic terminals (Wall et al., 2013; Guo et al., 2015).

However, when overlapping was observed, we discovered a different pattern between inputs to D1- vs. D2-MSNs. Interestingly, the proportions were reversed: more overlap was detected in the motor cortex of D2-Cre;Ai14 animals, whereas there were more pDMS-D1-expressing neurons in the cingular cortex projecting to D1-MSNs in the pDMS of D1-Cre;Ai14 animals (Tables 1-2). It is known that motor skills are acquired in the DMS during the initial formation of action-outcome associations (Yin et al., 2009). Motor behavior is affected by both D1- and D2-MSNs in the striatum; it has been suggested that both neuronal subtypes are coordinated to increase the wanted behavior (direct-pathway neurons) and decrease competing behaviors (indirect-pathway neurons) (Cui et al., 2013). Our data suggests that the D2-MSNs in the motor cortex are acting on pDMS-D2-MSNs; thus, increasing the strength of the inhibitory pathway and reducing competing behaviors can strengthen a specific association (mediated by the D1-

MSN-projecting pathway) in goal-directed behavior. The anterior cingular cortex has been hypothesized to differentiate various stimuli based on their association with a specific reward (Floresco et al., 2008). Our results suggest that the D1-MSNs in the cingular cortex project onto D1-MSNs in the pDMS to strengthen the association between a specific stimulus and reward, conversely, the inhibitory projections serve to decrease the association between other stimuli and the same reward.

We also observed limited overlap in the OFC of the D2-Cre;Ai14, but not the D1-Cre;Ai14 mice (Tables 1-2). It is known that the OFC is necessary for providing incentive values in goal-directed learning, and it projects to the DMS to mediate goal-directed activity (Ostlund and Balleine, 2007; Gremel et al., 2016). Our results suggest that the glutamatergic projections from the OFC to the pDMS mediate goal-directed learning by an inhibitory mechanism.

Remarkably, we did not observe any rabies-GFP-expressing neurons in the BLA of D1-Cre;Ai14 mice, but there was limited expression in D2-Cre;Ai14 mice (Figures 2-3). The BLA-pDMS connection is suggested to be involved in goal-directed learning by associating sensory and motivational outcomes (Corbit et al., 2013). It is known that the BLA projects to the pDMS using the traditional retrograde tracing method fluorogold (Corbit et al., 2013) and is innervated by more D1-MSN-projecting neurons from the DMS (Wall et al., 2013; Guo et al., 2015). Our results suggest that the BLA-pDMS connection is mediated by non-D2-MSNs, likely D1-MSNs, in the BLA projecting onto D2-MSNs in the pDMS.

Overall, the thalamus had more rabies-GFP-expressing neurons in D1-Cre;Ai14 animals, indicating that there are more non-D1R-expressing projections from the thalamus into the pDMS (Figures 2, 3). These non-D1R neurons are therefore likely to be D2R-expressing neurons, which is consistent with previous findings using the pseudorabies virus tracing (Wall et al., 2013; Guo et al., 2015). The thalamus expressed both pDMS-projecting D1- and D2-MSNs acting on pDMS D1- and D2-MSNs, respectively. There was substantially more overlap in the D2-MSNs than D1-MSNs in the thalamus-pDMS pathway (Tables 1, 2). Specific subregions of the thalamus have been shown to have a larger influence over the D2-expressing indirect-pathway neurons (Doig et al., 2010; Wall et al., 2013; Guo et al., 2015). However, we focused on the thalamus as a whole. Future analysis should be conducted to determine if and how the distinct subregions of the thalamus affect our observed overlap results. Nevertheless, it is important to note that there are cholinergic neurons that project from the thalamus to the pDMS that have been posited to play a role in associative learning by projecting to the cholinergic striatal interneurons (Bradfield et al., 2013; Guo et al., 2015; Yamanaka et al., 2017). These interneurons could have also been infected by the virus, causing rabies-GFP expression in thalamic neurons projecting onto pDMS interneurons.

This viral tracing method enables us to do very detailed circuit mapping, since the virus travels monosynaptically in a retrograde fashion. However, it is not without its limitations. First and foremost, we were only able to detect D1-MSNs (or D2-MSNs) in extrastriatal regions projecting directly onto D1-MSNs (or D2-MSNs) in the pDMS. This method is unable to distinguish D1-MSNs that project onto D2-MSNs, or D2-MSNs that project onto D1-MSNs, in the pDMS. These studies should be conducted using electrophysiological techniques.

Secondly, we noticed very limited overlap, which contrasted with our initial hypothesis. We explored the possibility of limited rabies-GFP expression by conducting immunohistochemistry using anti-GFP staining (data not shown). The staining did not affect our overlap percentages in the selected brain regions, indicating that restricted expression was most likely not the cause of low overlap. Another possibility for limited overlap could be due to variation in the infusion sites of RG/TVA and pseudotyped rabies because of the surgical procedure. The surgical protocol should be further refined for optimal results.

REFERENCES

Bolam JP, Hanley JJ, Booth PAC, Bevan MD (2000) Synaptic organisation of the basal ganglia. Journal of Anatomy 196:527-542.

Bradfield Laura A, Bertran-Gonzalez J, Chieng B, Balleine Bernard W (2013) The Thalamostriatal Pathway and Cholinergic Control of Goal-Directed Action: Interlacing New with Existing Learning in the Striatum. Neuron 79:153-166.

Cheng Y, Huang CCY, Ma T, Wei X, Wang X, Lu J, Wang J (2016) Distinct Synaptic Strengthening of the Striatal Direct and Indirect Pathways Drives Alcohol Consumption. Biological Psychiatry.

Corbit LH, Janak PH (2010) Posterior dorsomedial striatum is critical for both selective instrumental and Pavlovian reward learning. European Journal of Neuroscience 31:1312-1321.

Corbit LH, Leung BK, Balleine BW (2013) The Role of the Amygdala-Striatal Pathway in the Acquisition and Performance of Goal-Directed Instrumental Actions. The Journal of Neuroscience 33:17682-17690.

Cui G, Jun SB, Jin X, Pham MD, Vogel SS, Lovinger DM, Costa RM (2013) Concurrent activation of striatal direct and indirect pathways during action initiation. Nature 494:238-242.

Doig NM, Moss J, Bolam JP (2010) Cortical and Thalamic Innervation of Direct and Indirect Pathway Medium-Sized Spiny Neurons in Mouse Striatum. The Journal of Neuroscience 30:14610-14618.

Everitt BJ, Robbins TW (2005) Neural systems of reinforcement for drug addiction: from actions to habits to compulsion. Nat Neurosci 8:1481-1489.

Floresco SB, Onge JRS, Ghods-Sharifi S, Winstanley CA (2008) Cortico-limbic-striatal circuits subserving different forms of cost-benefit decision making. Cognitive, Affective, & Behavioral Neuroscience 8:375-389.

Gerfen CR, Surmeier DJ (2011) Modulation of striatal projection systems by dopamine. Annual review of neuroscience 34:441-466.

Gremel Christina M, Chancey Jessica H, Atwood Brady K, Luo G, Neve R, Ramakrishnan C, Deisseroth K, Lovinger David M, Costa Rui M (2016) Endocannabinoid Modulation of Orbitostriatal Circuits Gates Habit Formation. Neuron 90:1312-1324.

Guo Q, Wang D, He X, Feng Q, Lin R, Xu F, Fu L, Luo M (2015) Whole-Brain Mapping of Inputs to Projection Neurons and Cholinergic Interneurons in the Dorsal Striatum. PLoS ONE 10:e0123381.

Joel D, Weiner I (2000) The connections of the dopaminergic system with the striatum in rats and primates: an analysis with respect to the functional and compartmental organization of the striatum. Neuroscience 96:451-474.

Lee CR, Abercrombie ED, Tepper JM (2004) Pallidal control of substantia nigra dopaminergic neuron firing pattern and its relation to extracellular neostriatal dopamine levels. Neuroscience 129:481-489.

Lemberger T, Parlato R, Dassesse D, Westphal M, Casanova E, Turiault M, Tronche F, Schiffmann SN, Schütz G (2007) Expression of Cre recombinase in dopaminoceptive neurons. BMC Neuroscience 8:4-4.

Lovinger DM (2010) Neurotransmitter roles in synaptic modulation, plasticity and learning in the dorsal striatum. Neuropharmacology 58:951-961.

Madisen L, Zwingman TA, Sunkin SM, Oh SW, Zariwala HA, Gu H, Ng LL, Palmiter RD, Hawrylycz MJ, Jones AR, Lein ES, Zeng H (2010) A robust and high-throughput Cre reporting and characterization system for the whole mouse brain. Nat Neurosci 13:133-140.

Madisen L et al. (2012) A toolbox of Cre-dependent optogenetic transgenic mice for light-induced activation and silencing. Nat Neurosci 15:793-802.

Ostlund SB, Balleine BW (2007) The contribution of orbitofrontal cortex to action selection. Annals of the New York Academy of Sciences 1121:174-192.

Paxinos G, Franklin KB (2004) The mouse brain in stereotaxic coordinates: Gulf Professional Publishing.

Sacks JJ, Gonzales KR, Bouchery EE, Tomedi LE, Brewer RD (2015) 2010 National and State Costs of Excessive Alcohol Consumption. American Journal of Preventive Medicine 49:e73-e79.

Sano H, Yasoshima Y, Matsushita N, Kaneko T, Kohno K, Pastan I, Kobayashi K (2003) Conditional Ablation of Striatal Neuronal Types Containing Dopamine D2 Receptor Disturbs Coordination of Basal Ganglia Function. The Journal of Neuroscience 23:9078-9088.

Shiflett MW, Brown RA, Balleine BW (2010) Acquisition and Performance of Goal-Directed Instrumental Actions Depends on ERK Signaling in Distinct Regions of Dorsal Striatum in Rats. The Journal of Neuroscience 30:2951-2959.

Sippy T, Lapray D, Crochet S, Petersen Carl CH (2015) Cell-Type-Specific Sensorimotor Processing in Striatal Projection Neurons during Goal-Directed Behavior. Neuron 88:298-305.

Smith Y, Raju DV, Pare J-F, Sidibe M (2004) The thalamostriatal system: a highly specific network of the basal ganglia circuitry. Trends in Neurosciences 27:520-527.

Stahre M, Roeber J, Kanny D, Brewer RD, Zhang X (2014) Contribution of Excessive Alcohol Consumption to Deaths and Years of Potential Life Lost in the United States. Preventing Chronic Disease 11:E109.

Surmeier DJ, Ding J, Day M, Wang Z, Shen W (2007) D1 and D2 dopamine-receptor modulation of striatal glutamatergic signaling in striatal medium spiny neurons. Trends in Neurosciences 30:228-235.

Taverna S, Ilijic E, Surmeier DJ (2008) Recurrent collateral connections of striatal medium spiny neurons are disrupted in models of Parkinson's disease. The Journal of neuroscience : the official journal of the Society for Neuroscience 28:5504-5512.

Tepper JM, Abercrombie ED, Bolam JP (2007) Basal ganglia macrocircuits. In: Progress in Brain Research (James M. Tepper EDA, Bolam JP, eds), pp 3-7: Elsevier.

Tricomi E, Balleine BW, O'Doherty JP (2009) A specific role for posterior dorsolateral striatum in human habit learning. European Journal of Neuroscience 29:2225-2232.

Volkow Nora D, Morales M (2015) The Brain on Drugs: From Reward to Addiction. Cell 162:712-725.

Voorn P, Vanderschuren LJMJ, Groenewegen HJ, Robbins TW, Pennartz CMA (2004) Putting a spin on the dorsal–ventral divide of the striatum. Trends in Neurosciences 27:468-474.

Wall Nicholas R, De La Parra M, Callaway Edward M, Kreitzer Anatol C (2013) Differential Innervation of Direct- and Indirect-Pathway Striatal Projection Neurons. Neuron 79:347-360.

Wang J, Lanfranco MF, Gibb SL, Yowell QV, Carnicella S, Ron D (2010) Long-Lasting Adaptations of the NR2B-Containing NMDA Receptors in the Dorsomedial Striatum Play a Crucial Role in Alcohol Consumption and Relapse. The Journal of Neuroscience 30:10187-10198.

Wang J, Cheng Y, Wang X, Roltsch Hellard E, Ma T, Gil H, Ben Hamida S, Ron D (2015) Alcohol Elicits Functional and Structural Plasticity Selectively in Dopamine D1 Receptor-Expressing Neurons of the Dorsomedial Striatum. The Journal of Neuroscience 35:11634-11643.

Wei X, Ma T, Cheng Y, Huang CCY, Wang X, Lu J, Wang J (2017) Dopamine D1 or D2-receptor expressing neurons in the central nervous system. Addiction Biology Accepted.

Wickersham IR, Lyon DC, Barnard RJ, Mori T, Finke S, Conzelmann KK, Young JA, Callaway EM (2007) Monosynaptic restriction of transsynaptic tracing from single, genetically targeted neurons. Neuron 53:639-647.

Williams ZM, Eskandar EN (2006) Selective enhancement of associative learning by microstimulation of the anterior caudate. Nat Neurosci 9:562-568.

Yamanaka K, Hori Y, Minamimoto T, Yamada H, Matsumoto N, Enomoto K, Aosaki T, Graybiel AM, Kimura M (2017) Roles of centromedian parafascicular nuclei of thalamus and cholinergic interneurons in the dorsal striatum in associative learning of environmental events. Journal of Neural Transmission:1-13.

Yin HH, Knowlton BJ, Balleine BW (2005) Blockade of NMDA receptors in the dorsomedial striatum prevents action–outcome learning in instrumental conditioning. European Journal of Neuroscience 22:505-512.

Yin HH, Mulcare SP, Hilario MRF, Clouse E, Holloway T, Davis MI, Hansson AC, Lovinger DM, Costa RM (2009) Dynamic reorganization of striatal circuits during the acquisition and consolidation of a skill. Nat Neurosci 12:333-341.

FIGURES

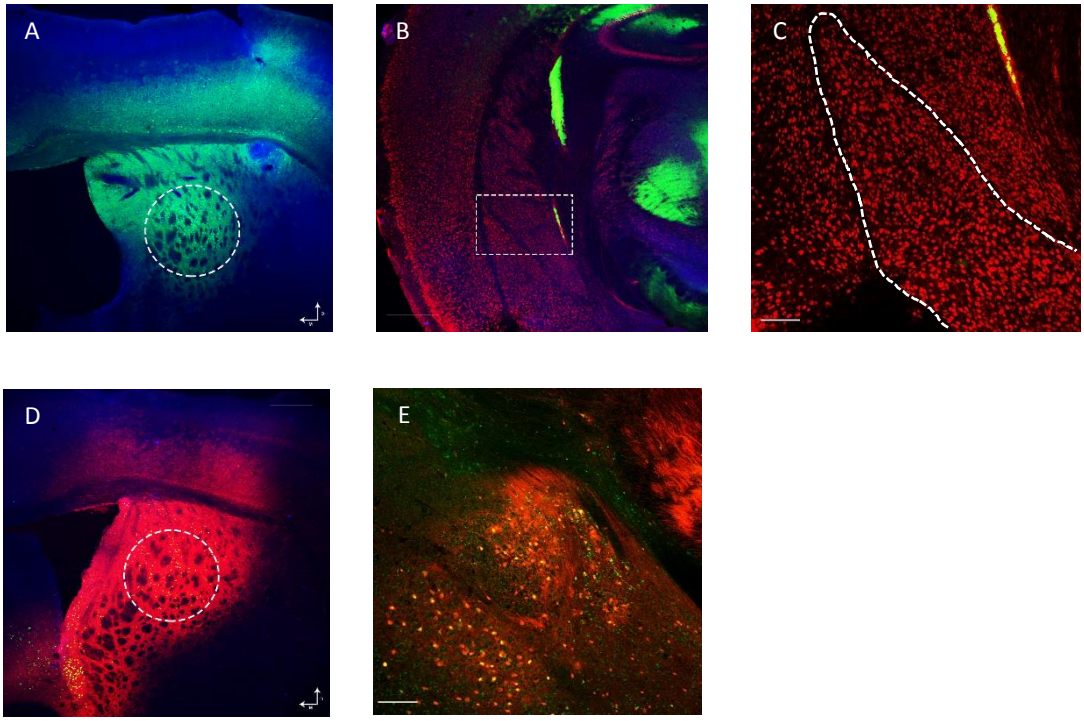

Figure 1: Verification of the pDMS infusion site of AAV2.5-Cre-eGFP. AAV2.5-Cre-GFP was infused into the pDMS of Ai32 (express ChR2-GFP after Cre recombination, A-C) and Ai14 (express tdTomato after Cre recombination, D-E) mice at coordinates of AP, 0.0; ML, ±1.87; DV, -2.9. The AAV2.5-Cre infected pDMS neurons, as well as axon terminals of neurons that project to the pDMS. The axon-infected AAV2.5-Cre-eGFP was retrogradely transported along the axon to the soma located outside the striatum. A) Fluorescent image of a coronal section of the pDMS infusion site in an Ai32 mouse. A large amount of green neurons were observed in the pDMS (dashed area) and few were detected in the cortex. Scale bar, 300 µm. B) No GFP-positive neurons were found in the BLA of an Ai32 mouse. Scale bar, 500 µm. C) Magnified image of B (boxed region) showing no pDMS-projecting neurons in the BLA of an Ai32 mouse.

Scale bar, 150 µm. D) Fluorescent image of a coronal section of the pDMS infusion site in an Ai14 mouse showing strong red neurons in the pDMS. Scale bar, 400 µm. E) pDMS-projecting neurons in the BLA of the Ai14 mouse. Scale bar, 150 µm.

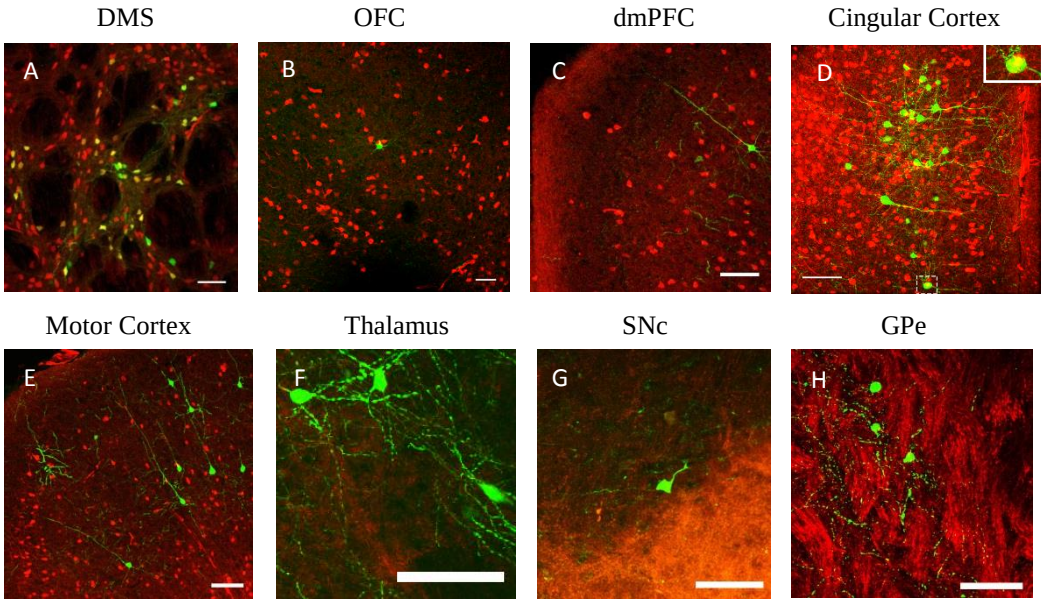

Figure 2: D1-MSNs receive strong projections from a variety of cortical areas, thalamus, SNc, and GPe. AAV8-Flex-RG and AAV8-Flex-TVA-mCherry were infused into the pDMS of six female D1-Cre;Ai14 mice at the following coordinates: AP, 0.0 mm; ML, ± 1.87 mm; DV, -2.90 mm. After allowing four weeks for expression, EnvA-SADΔG-EGFP pseudorabies virus was infused at a 10-degree angle to prevent coincident infection at the adapted coordinates AP, 0.0 mm; ML, ± 2.42 mm; DV, -2.94 mm. Sample images were taken in several regions: A) pDMS expresses D1-MSNs (red) and rabies-GFP neurons (green), and pDMS D1-MSN-projecting neurons (yellow). Scale bar, 50 µm. B) Limited rabies-GFP expression was detected in the OFC. Scale bar, 50 µm. C) Red and green neurons were observed in the dmPFC. Scale bar, 80 µm. D) The cingular cortex expressed several rabies-GFP neurons and overlap with D1-MSNs (inset). Scale bar, 70 µm. E) Motor cortex had limited rabies-GFP expression. Scale bar, 100 µm. F) Thalamus expressed several rabies-GFP neurons. Scale bar, 80 µm. G) SNc expresses red D1-MSNs and few green neurons. Scale bar, 50 µm. H) GPe expresses mostly red fibers with some rabies-GFP neurons. Scale bar, 80 µm.

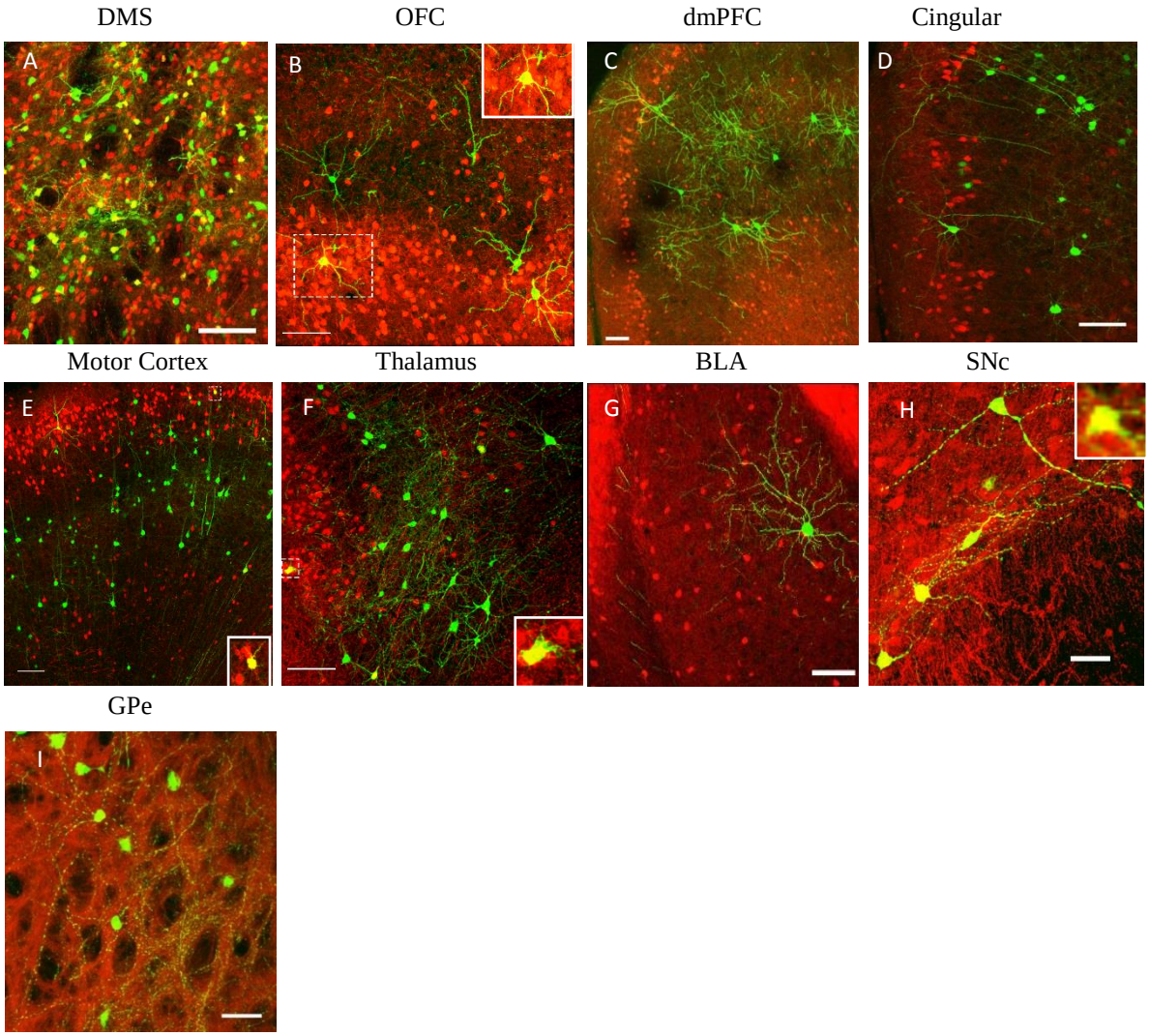

Figure 3: D2-MSNs receive strong projections from a variety of cortical areas, thalamus, BLA, SNc, and GPe. Four D2-Cre;Ai14 mice (three female, one male) were infused in the same manner as stated in Figure 2. Sample images were taken in several regions: A) pDMS expresses D2-MSNs (red) and rabies-GFP neurons (green), and many pDMS D2-MSN-projecting neurons (yellow). Scale bar, 50 µm. B) Several rabies-GFP-expressing neurons as well as limited overlap were detected in the OFC (inset). Scale bar, 100 µm. C) Red and green neurons were observed in the dmPFC. Scale bar, 80 µm. D) The cingular cortex expressed several rabies-GFP neurons. Scale bar, 100 µm. E) Motor cortex expressed many rabies-GFP

neurons and overlap was detected (inset). Scale bar, 100 µm. F) Thalamus expressed several rabies-GFP neurons and overlap was detected (inset). Scale bar, 100 µm. G) A rabies-GFP neuron was detected in the BLA. Scale bar, 80 µm. H) SNc expresses red D2-MSNs and few green neurons with several overlapping (inset). Scale bar, 50 µm. I) GPe expresses mostly red fibers with several rabies-GFP neurons. Scale bar, 80 µm.

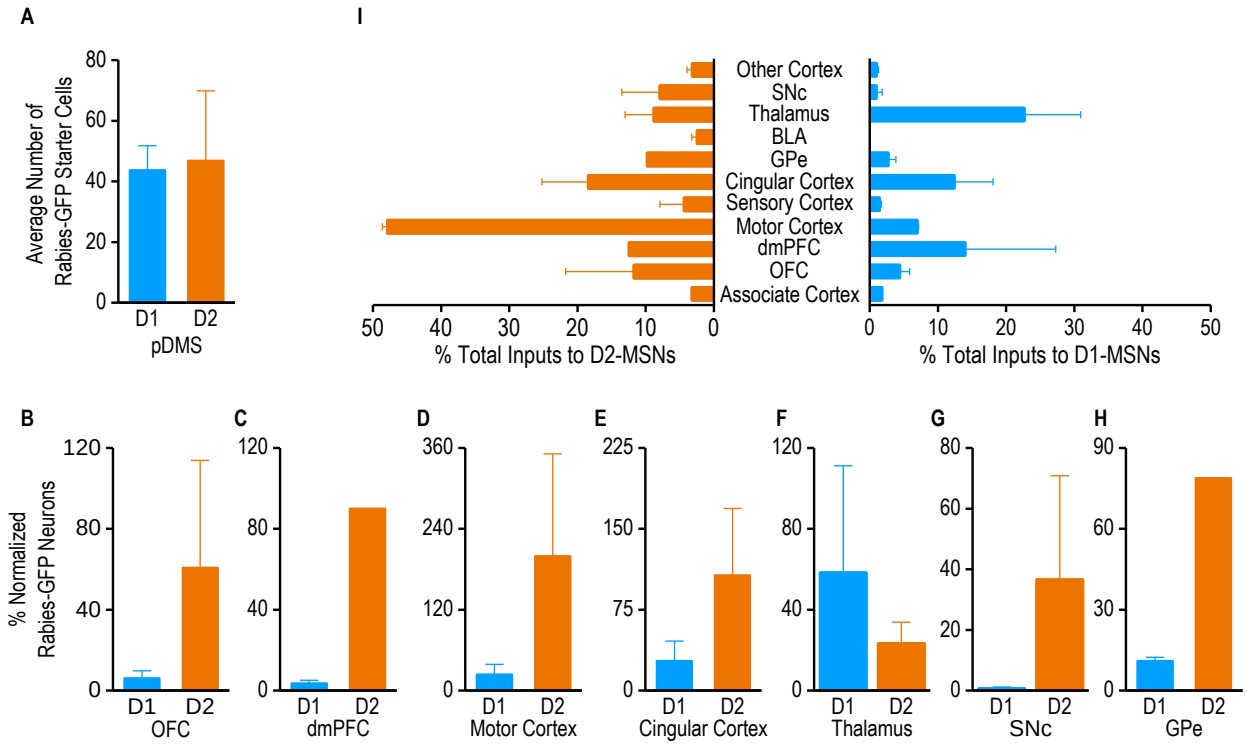

Figure 4: Summary of the percentage of normalized rabies GFP-expressing neurons in each region to the percentage of the total inputs to D1- and D2-MSNs. The percentage of total inputs from each brain region into the pDMS was calculated for D1-MSNs and D2-MSNs (I). All data is expressed as the mean ± SE. A) Average numbers of rabies-GFP starter cells in the pDMS. n = 24 sections from 4 mice for D1-MSNs and 21 sections from 3 mice for D2-MSNs. B-H) Bar graphs comparing normalized inputs to D1- vs. D2-MSNs in different brain regions. The number of starter cells in the pDMS were used to normalize the results of rabies-GFP expression in each brain region, expressed as a percentage. n = 7 sections, 2 mice (OFC, D1-MSNs); 10, 3 (OFC, D2-MSNs); 12, 2 (dmPFC, D1-MSNs); 5, 1 (dmPFC, D2-MSNs); 21, 3 (motor cortex, D1-MSNs); 27, 2 (motor cortex, D2-MSNs); 16, 3 (cingular cortex, D1-MSNs); 13, 3 (cingular cortex, D2-MSNs); 13, 2 (thalamus, D1-MSNs); 10, 2 (thalamus, D2-MSNs); 2, 2 (SNc, D1-MSNs); 9, 2 (SNc, D2-MSNs); 10, 2 (GPe, D1-MSNs); 4, 1 (GPe, D2-MSNs). I)

Percentage of total inputs to D1-MSNs (right) and D2-MSNs (left) in multiple brain regions. The sample sizes are the same as Figure 4B-4H. n = 4, 2 (Other cortex regions, D1-MSNs); 6, 2 (Other cortex regions, D2-MSNs); 9, 2 (BLA, D2-MSNs); 6, 3 (sensory cortex, D1-MSNs); 3, 2 (sensory cortex, D2-MSNs); 1, 1 (associate cortex, D1-MSNs); 2, 1 (associate cortex, D2-MSNs).

TABLES

Table 1: Summary of D1R-positive and rabies-positive neurons in key regions examined.

	$D1^+$	$Rabies^+$	$D1^+$+$Rabies^+$	Overlap*
DMS	5486.8 ± 2504.8	286.0 ± 129.3	114.0 ± 63.5	43.7 ± 8.1
Associate cortex	176.0	1.0	0.0	0.0
OFC	432.0 ± 139.5	2.3 ± 0.3	0.0 ± 0.0	0.0 ± 0.0
dmPFC	614.0 ± 279.0	8.0 ± 7.0	0.0 ± 0.0	0.0 ± 0.0
Motor Cortex	1470.7 ± 812.6	20.0 ± 13.6	0.3 ± 0.3	0.7 ± 0.7
Cingular Cortex	871.3 ± 209.1	25.7 ± 15.8	1.0 ± 1.0	1.8 ± 1.8
BLA	0.0 ± 0.0	0.0 ± 0.0	0.0 ± 0.0	0.0 ± 0.0
Thalamus	73.0 ± 70.0	58.0 ± 41.0	0.5 ± 0.5	0.5 ± 0.5
Sensory Cortex	412.7 ± 304.6	3.3 ± 1.9	0.0 ± 0.0	0.0 ± 0.0
SNc	0.0 ± 0.0	1.0 ± 0.0	0.0 ± 0.0	0.0 ± 0.0
GPe	45.5 ± 20.5	8.0 ± 3.0	0.0 ± 0.0	0.0 ± 0.0
Other cortex	17.5 ± 17.5	5.0 ± 4.0	0.0 ± 0.0	0.0 ± 0.0

*Overlap: $D1^+$ + $Rabies^+$/ $Rabies^+$

Table 2: Summary of D2R-positive and rabies-positive neurons in key regions examined.

	$D2^+$	$Rabies^+$	$D2^+$+$Rabies^+$	Overlap*
DMS	1039.67 ± 971.01	293.00 ± 134.31	75.33 ± 28.39	46.81 ± 23.04
Associate cortex	0.00	4.00	0.00	0.00
OFC	308.67 ± 291.78	17.67 ± 11.46	1.00 ± 1.00	2.50 ± 2.50
dmPFC	2034.00	72.00	0.00	0.00
Motor Cortex	795.00 ± 666.00	169.50 ± 111.50	2.00 ± 2.00	0.71 ± 0.71
Cingular Cortex	245.00 ± 245.00	69.33 ± 53.96	0.67 ± 0.67	0.38 ± 0.38
BLA	174.50 ± 174.50	7.00 ± 3.00	0.00 ± 0.00	0.00 ± 0.00
Thalamus	47.50 ± 41.50	21.50 ± 5.50	4.50 ± 1.50	24.31 ± 13.19
Sensory Cortex	0.00 ± 0.00	5.50 ± 4.50	0.00 ± 0.00	0.00 ± 0.00
SNc	1.00 ± 1.00	10.00 ± 7.00	1.00 ± 1.00	5.88 ± 5.88
GPe	122.00	63.00	0.00	0.00
Other cortex	0.00 ± 0.00	4.00 ± 2.00	0.00 ± 0.00	0.00 ± 0.00

*Overlap: $D2^+$ + $Rabies^+$/ $Rabies^+$